Experimental and numerical investigation of the water-entry and water-exit of a circular cylinder

G.Colicchio[1,2] , M.Greco[1,2] , M.Miozzi[1] , C.Lugni[1,2]

1 **INSEAN, Italian Ship Model Basin, Roma – Italy.**
2 **Centre for Ships and Ocean Structures (CeSOS), NTNU, Trondheim – Norway.**

The water entry of a body is a very important topic in naval hydrodynamic. This phenomenon plays an important role both for offshore structures and for vessels. High forward speed of the vessel and rough head sea states usually lead to the most severe water entry events. In such circumstances, the wave-body interactions may result in pronounced motions of the vessel with largest amplitudes at the bow region. In this area, the probability of water entry is the largest, i.e. portions of the hull can more easily touch the sea surface at high relative velocity. The water-entry phenomenon is intrinsically a transient phase. Its beginning can be characterized by highly localized, both in space and in time, loads on the vessel, influencing both the local structural safety of the ship and the global loads acting on the ship itself.
The occurrence and involved features depend on the body geometry (bluntness, presence of sharp variations, flare, asymmetries; etc.), its operational conditions (ballast, loaded; fixed, moored, with forward speed; etc.) and the sea state. The severity and the effects are also strongly dependent on the local shape of the ship and of the sea surface interested by the impact, on their relative velocity, on the initial liquid flow and on the properties of the solid surface.
Among the problems connected with the transient phases occurring during marine operations, the water-exit phenomenon is one of the less studied and known. With such term one refers to the circumstances where a partially or fully immersed body exits the water. This means that it can interest both offshore platforms, i.e. during lifting operations of submarine modules with cranes, and submarine vehicles.
Even though these problems can rise such a broad interest, most of the studies are still limited to the fundamental research, where the analysis is carried out on simplified shapes. More commonly they are limited to 2D sections with circular or triangular shapes.
Experiments with rigid circular cylinders falling onto an initially calm water were already carried out in [1-2-3-4-5]. Either forced motions (with constant entry speed) or free-falling scenarios were considered. Some study recorded the flow evolution, some measured the vertical force or the pressure time history. As relevant features, an initial transient phase of short duration associated with peaked loads and a later flow separation were documented. A fundamental study on the water exit of a circular, initially fully immersed, cylinder was performed in [4]. His 2D calm-water model tests highlighted an accelerated phase after the cylinder release and then a stage with nearly constant rising speed. Forced water exit (with constant exit speed) were examined in [2]. In both cases the physical investigation was based on video recording of the tests.
As relevant features, wide disturbances of the free surface and possible occurrence of cavitation where noted.
Here an experimental and numerical analysis is performed for a circular cylinder either freely falling on or exiting the water. From the experimental point of view, a detailed measurement of the velocity field and of the local loads around the cylinder is carried out.

Experimental set up The experiments were conducted in a prismatic tank with the following geometrical characteristics: length 3000mm, width 400mm and depth 1400mm (see Figure 1). The tank is entirely realized in Plexiglas (40mm thick) and crystal glass to allow the optical accessibility in each direction.

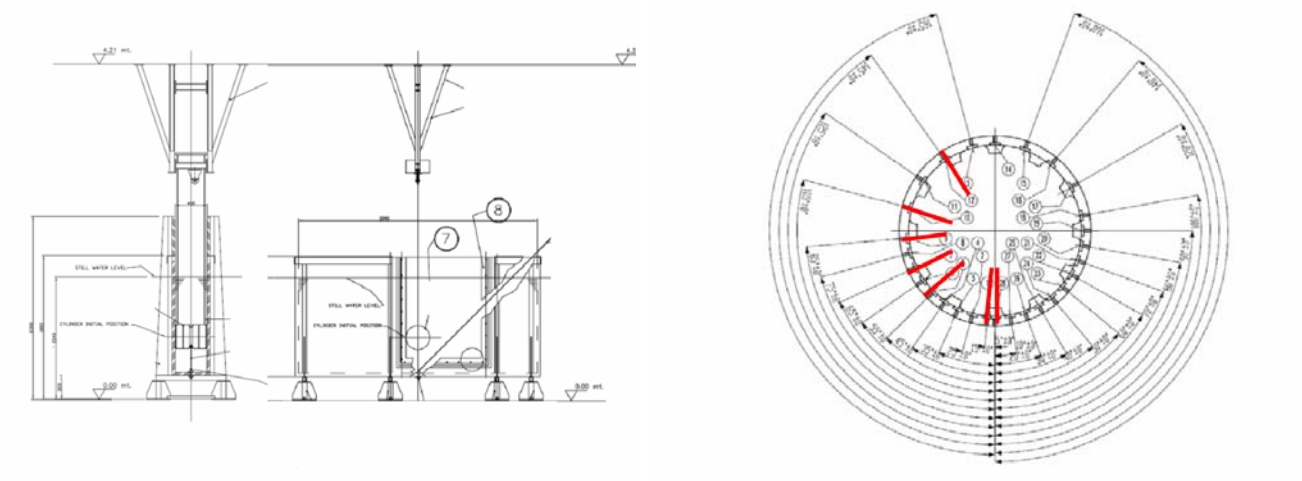

Figure 1: Sketch of the tank (left) and of the cylinder with the positions of the pressure transducers (right).
The tank is anchored to the ground with a mechanism completely separated from the one supporting the cylinder. In this way the coupling between the entering/exiting body and the water is only possible through hydrodynamic actions.
The mechanism releasing the cylinder and guiding it in its motions has been realized so to have the structural frequencies as far as possible from the ones characterizing the hydrodynamic loads.
The release of the cylinder is regulated by a magnet driven by a trigger signal. The last one is recorded in the acquisition system and used as a synchronization signal. The cylinder is in stainless steel with a diameter of 30cm.
The central section is provided of holes for the pressure transducers. Their positions on the cylinder are represented in Figure 1. The cables of the transducers exit the cylinder from a hole in the upper part of it. Its presence on one side of the cylinder can mine the symmetry of the flow. Two absolute pressure transducers ENDEVCO 8510C (max measurable pressure 50Psi) are used in the bottom

positions, respectively at 0° and 15° (see Figure 1). Five relative pressure transducers Kulite XLC-072 with (max measurable pressure 5 Psi) are positioned in the upper holes of the cylinder at the angles 45°, 65°, 85° , 105° and 145° (see Figure 1). The vertical motion and velocity of the falling body is measured through a wire potentiometer with one end of the wire fixed to the roof and the other one to the falling cylinder. A High frequency acquisition system NI-PXI is used to record all the signals at a sample rate of 16 kHz. The velocity field around the cylinder is investigated through a PTV methodology. The images are recorded by the fast videocamera PHOTRON with a frame rate of 1 kfps and a spatial resolution equal to 1024x1024 pixels. The flow field has been seeded with ceramic spherical particles with radius O(100) micron illuminated by a diffused fluorescent light.

Numerical method The numerical investigation is carried on with a two-phase Navier-Stokes solver based on an approximated projection method. The equations are discretized on a Cartesian staggered grid with a second order approximation both in time and space. The body is approximated on the Cartesian grid with a level-set function as well as the air-water interface. For more details see [6] and [7].

Water entry problem A cylinder, of weight W_b equal to 0.62 times the weight of the water it displaces W_w, is released from a height of 0.48m from the free surface. Due to the friction on the guides and to the elastic restoring force of the wire potentiometer, the entry velocity is approximately equal to V_e=2.55m/s, smaller than the theoretical prediction $V_{eT}=(2gh)^{0.5}$ = 3.06 m/s. To reduce unavoidable differences between numerics and experiments, the measured entry velocity is given as input to the Navier-Stokes solver. The trajectory of the bottom of the cylinder and its velocity are plotted in Figure 2. The experimental data are plotted with the error bars, calculated with the standard deviation of 9 repeated runs; the numerical results are represented with a continuous line with circular bullets.

Here only the entry phase will be analyzed and it finishes at t=0.4s. Nonetheless the plots report longer times to give more complete information. In $t \in [0.0s,0.4s]$ the comparison is satisfactory; for longer times, the differences between the two data sets increase because of the elastic restoring force of the wire potentiometer, not taken into account in the numerical simulation.

When the body enters the water, it causes a pressure impulse. This can be seen in the numerical and experimental pressure records at the three lower sensors (see Figure 3). The amplitude of the impulse is different in the two records but both of them are influenced by the integration area, equal to the grid size in the numerical data and to the area of the sensor in the experiments. However, its time-length is comparable and of the size of 2ms (see second upper plot of Figure 3). There, the pressure peak is preceded by a gentle increase, that is caused by the dynamic action of the air entrapped between the cylinder and the free surface just before the impact.

While the body enters the water the sensors up to 65° are quickly wetted, the upper ones are wetted only once the cylinder slows down and the jets, created at its sides, fall down on it (see Figure 4).

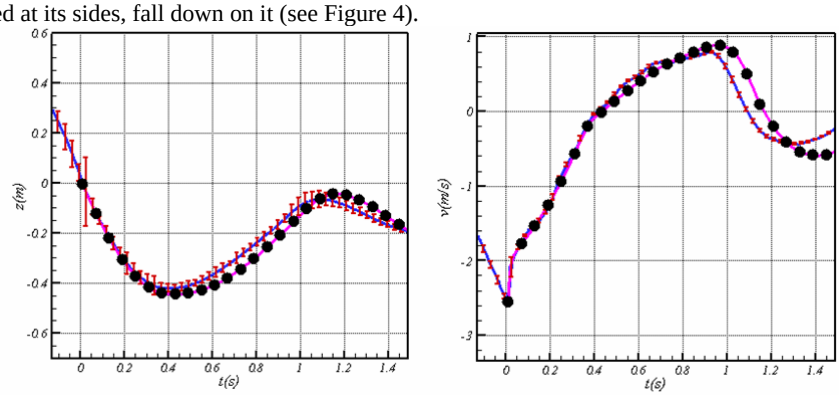

Figure 2: Water entry: position (left) and velocity (right) of the bottom of the cylinder. Experiments: lines with error bars, numerics: lines with bullets. (t=0.0s corresponds to the impact).

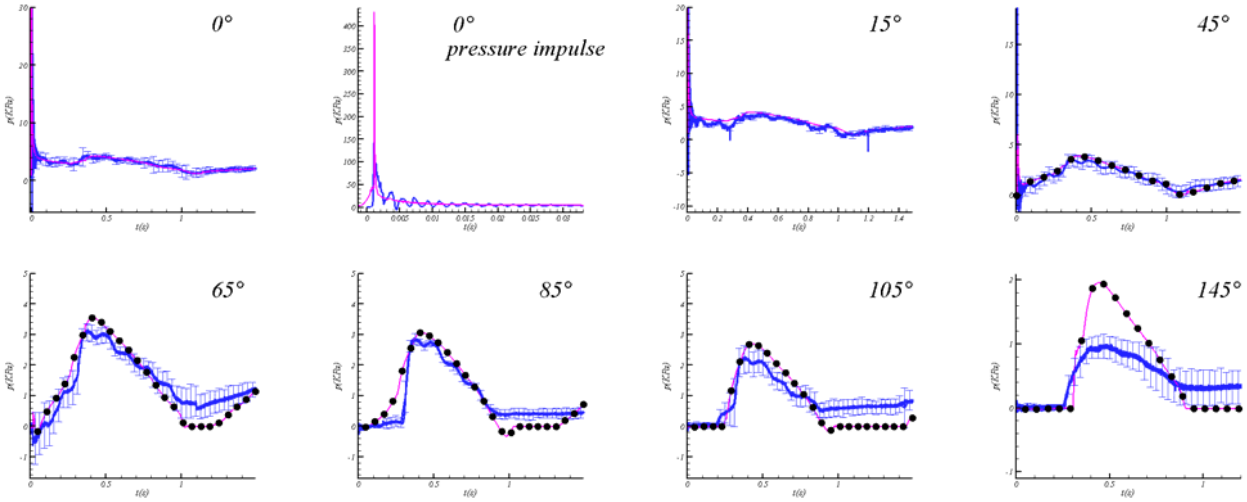

Figure 3: Water-entry: Pressures at the positions in Figure 1.

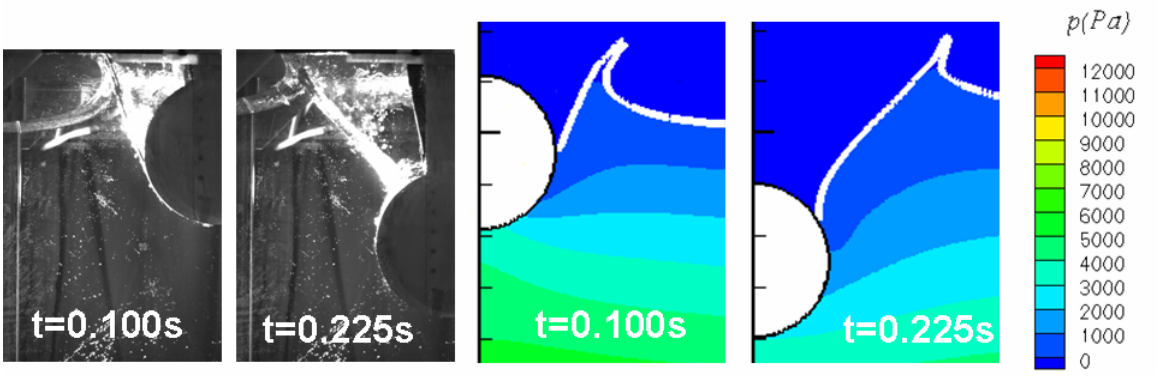

Figure 4: Water entry of a light cylinder. Experimental images (left side) and numerical simulations (right side).

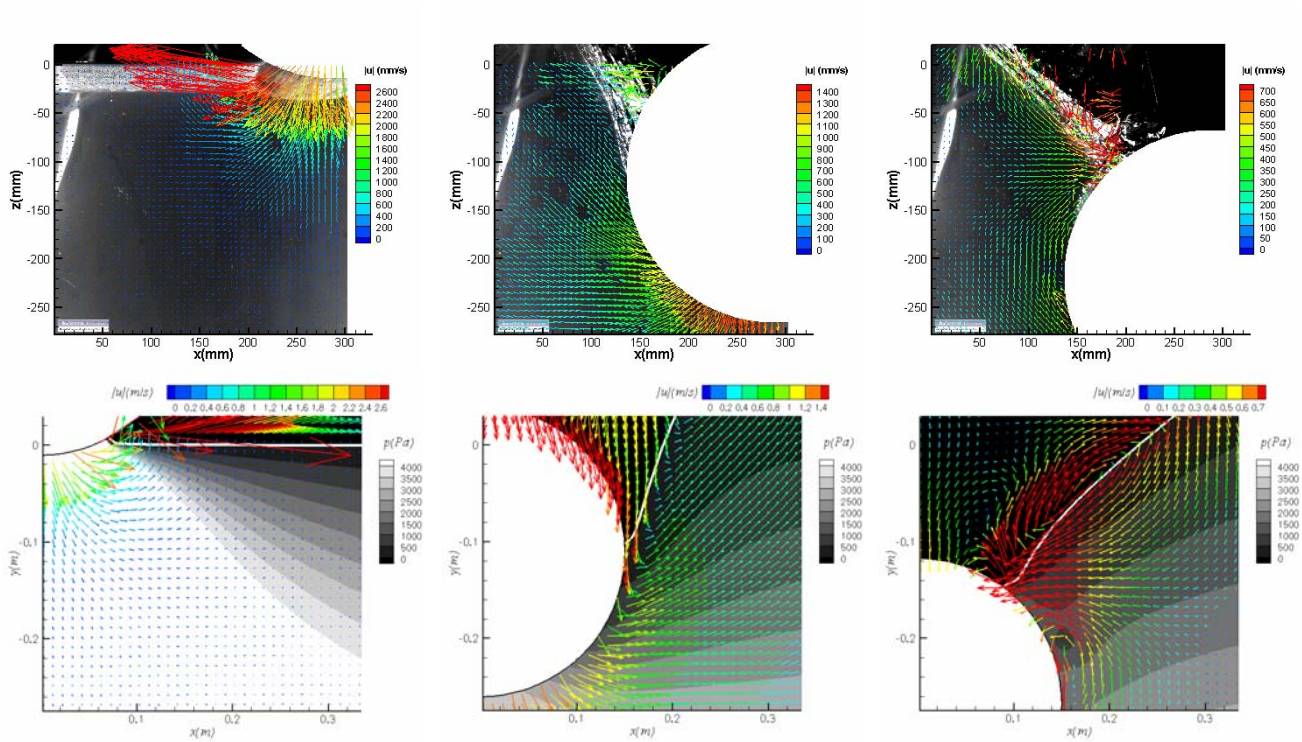

Figure 5: Water entry. Top: PTV images of the water entry phase of the cylinder. Bottom: Numerical predictions of velocity and pressure. From left to right the times are t= 0.004s, 0.154s, 0304s.

Figure 5 shows the experimental (top panels) and numerical (bottom panels) velocity field around the entering body at three characteristic time instants: 1) at the impact time, when the flow velocity is similar to the impact speed only in the region close to the cylinder, the numerical pressure contours highlight the effects of the fading pressure impulse; 2) at the time instant of the steady jet formation, when the angle of detachment of the jet does not change in time, 3) at the time instant when the jet falls on the body and closes on it, this generates a local low pressure region.

Water exit problem The same cylinder described above is immersed with its centre at a depth of 0.46m from the undisturbed free surface. Because of its buoyancy, it rises causing the deformation of the free surface until it finally exits the free surface.

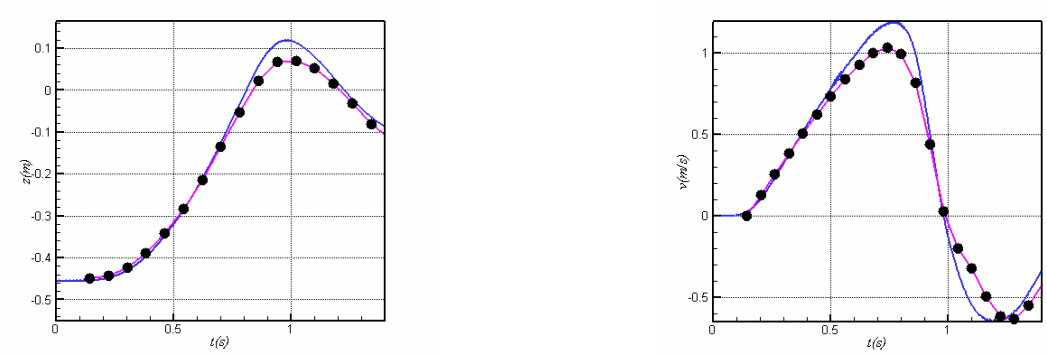

Figure 6: Water-exit. Position and velocity of the centre of the cylinder. Experiments: solid line, numerics: lines with bullets.

The position of the cylinder and its velocity are plotted in Figure 6. The real exiting phase finishes at t=1.s, afterwards, the cylinder falls down again because of its weight. Contrarily to what happened in the water-entry phase, the maximum position and the

maximum exit velocity predicted by the numerical solver is lower than the one recorded in the experiments. This confirms the restoring effect of the position transducer.
During its upward motion, the cylinder both deforms the free surface and creates a wake behind it. The core of the wake is characterized by low pressure which causes the entrapment of the bubbles normally dispersed in water. So that when the vorticity interacts with the body, the bubbles in it cause noise on the experimental pressure records (see Figure 8).

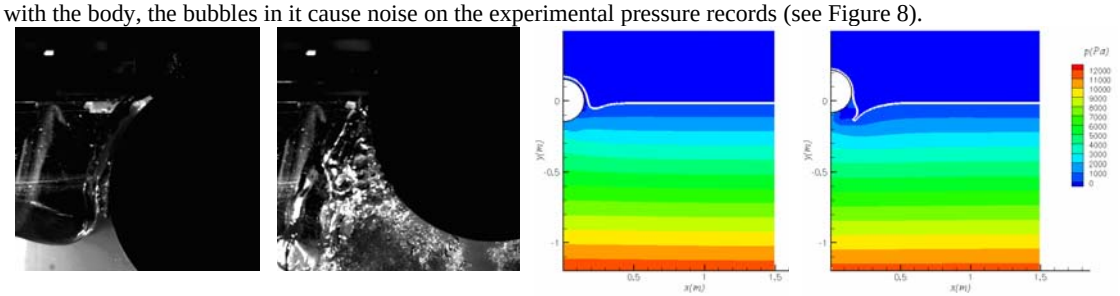

Figure 7: Water exit of a light cylinder. Experimental images (left side) and numerical simulations (right side). The figures correspond to the times t=0.682s, t=0.820s.
The trapped bubbles are evident in the experimental images of Figure 7. There, a population of bubbles fills the areas marked by negative pressure in the numerical computation. At the time corresponding to the first image, t=0.682s, the pressure probe at 105° (see Figure 8) is affected by a drop caused by the vortex core coincident with the bubble appearing in figure. Its disappears at t=0.82s, when the probe is dry. Figure 8 shows that the bottom probes at 0°-15°-45° are always wet, even at $t \geq 0.82$s, this means that the wake is always present even though composed by a mixture of water and air bubbles . The latter are driven there by the low pressure caused by the vorticity.

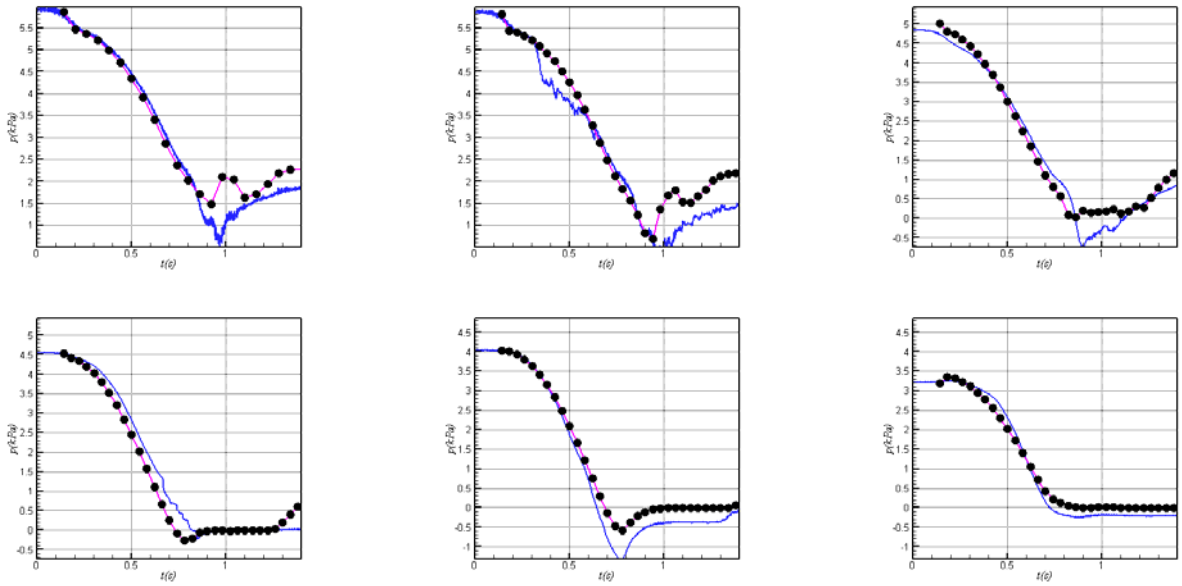

Figure 8: Water-exit. Pressures records at the angles 0°, 15°, 45°, 85°, 105° and 145°. Experiments: solid line, numerics: lines with bullets.
This research activity is partially supported by the Centre for Ships and Ocean Structures (CeSOS), NTNU, Trondheim, within the “Violent Water-Vessel Interaction and Related Structural Loads” project, partially supported by the Italian Navy within the “6-dof RANSE” project and partially done within the framework of the “Programma di Ricerca sulla Sicurezza” funded by Ministero Infrastrutture e trasporti.

References
[1] O.M. Faltinsen, O. KjÃrland, A. NÃttveit and T. Vinje, 1977,Water impact loads and dynamic responce of horizontal circular cylinder in offshore structures, Proc. Offshore Technology Conference, 119-126.
[2] G.Miao, 1989, Hydrodynamic forces and dynamic responses of circular cylinders in wave zones, Dept. Marine Hydrodynamics, NTH, Trondheim, Norway.
[3] K. Hagiwara, T. Yuhara, 1974,Fundamental study of wave impact load on a ship bow, J. Soc. Naval Arch. Japan, 135, 181-189.
[4] M. Greenhow, W.-M. Lin, 1983, Non--linear free surface effects: experiments and theory, Dept. Ocean Engng. Cambridge, 83--19, Mass: Mass. Inst. Technol.
[5] I.M.C. Campbell, P.A. Weynberg, 1980, Measurement of parameters affecting slamming, Wolfson Unit of Marine Technology, Tech. Rep. Centre, 440, Southampton, UK.
[6] G. Colicchio, M. Landrini, J.R. Chaplin, 2005, Level-set Computations of Free Surface Rotational Flows.Journal of Fluids Engineering, 127(6), p. 1111-1121
[7] G. Colicchio, M.Greco and O.M. Faltinsen, 2006, Fluid-body interaction on a Cartesian grid: dedicated studies for a CFD validation, Proc. WWWFB, Loughbrough, UK.